Supporting Information for

Selectivity in the initial C-H bond cleavage of n-butane on PdO(101)

Can Hakanoglu(a), Feng Zhang(a), Abbin Antony(a), Aravind Asthagiri(b) and Jason F. Weaver(a)*

(a) Department of Chemical Engineering, University of Florida, Gainesville, FL 32611, USA
(b) William G. Lowrie Department of Chemical and Biomolecular Engineering, The Ohio State University, Columbus, OH, 43210, USA

Quantification of Bond Selectivity

To quantify the C-H bond selectivity of n-butane on PdO(101), we analyzed our data within the context of a kinetic model developed by Weinberg and Sun,[1] after modifying the model to more accurately represent the experimental conditions employed in our study. The model describes the kinetics for the precursor-mediated dissociation of an alkane on a solid surface, wherein a molecularly-adsorbed state of the alkane serves as the precursor for dissociation and a kinetic branching between desorption and dissociation determines the net dissociation probability. The following reactions represent the elementary steps that are considered in the model,

$$CH_3CH_2CH_2CH_3\,(g) \rightleftharpoons CH_3CH_2CH_2CH_3\,(ad) \qquad k_d$$

$$CH_3CH_2CH_2CH_3\,(ad) \rightarrow CH_3CH_2CH_2CH_2\,(ad) + H(ad) \qquad k_{1H}$$

$$CH_3CH_2CH_2CH_3\,(ad) \rightarrow CH_3CHCH_2CH_3\,(ad) + H(ad) \qquad k_{2H}$$

The first step depicts the reversible adsorption of n-butane into the molecularly-adsorbed precursor state where k_d represents the rate coefficient for desorption. The remaining steps represent the dissociation of adsorbed n-butane by either 1° or 2° C-H bond cleavage with the rate coefficients for these steps denoted as k_{1H} and k_{2H}, respectively. These "apparent" rate coefficients implicitly take into account the different number of 1° vs. 2° C-H bonds in the n-butane molecule. According to the model, the total probability for dissociative chemisorption of n-butane (d_0) in the limit of zero coverage is given by,

$$S_0 = \frac{\alpha(k_{1H} + k_{2H})}{k_{1H} + k_{2H} + k_d} = \frac{\alpha k_{r0}}{k_{r0} + k_d} \qquad (1)$$

where α is the molecular adsorption probability and $k_{r0} = k_{1H} + k_{2H}$. The quantity k_{r0} represents an effective rate coefficient for the initial dissociation ("reaction") of n-butane-d_0. By analogy, the effective dissociation rate coefficients for the d_6 and d_{10} species are given by the equations, $k_{r6} = k_{1D} + k_{2H}$ and $k_{r10} = k_{1D} + k_{2D}$, where k_{1D} and k_{2D} represent the rate coefficients for primary and secondary C-D bond cleavage, respectively. These definitions assume that the rate coefficients for primary and secondary C-H(D) bond cleavage are independent of the isotopologue, e.g., k_{1D} is the same for both n-butane-d_6 and d_{10}. In the analysis, we also assume that the desorption rate coefficients and molecular adsorption probabilities are the same for the different n-butane isotopologues. We define a branching ratio for isotopologue d_j as

$$f_j = \frac{k_{rj}}{k_d} \qquad (2)$$

where the branching ratio is related to the dissociation probability by the equation,

$$f_j = \frac{S_j}{\alpha - S_j} \qquad (3)$$

The main goal of the analysis is to quantify the probabilities for 1° vs. 2° C-H bond cleavage from experimental measurements of the reactivity of different n-butane isotopologues. Toward this end, one may define the apparent probability for 1° C-H bond cleavage p_1 as equal to a kinetic branching probability by the equations,

$$p_1 = \frac{k_{1H}}{k_{1H} + k_{2H}} \cong \frac{k_{1D}}{k_{1D} + k_{2D}} \qquad (4)$$

The quantity p_1 represents the probability for 1° C-H bond cleavage, given that n-butane reacts, and is also equal to the fraction of the butyl products that are 1-butyl groups. Equation (4) assumes that the relation $k_{1H}/k_{2H} \cong k_{1D}/k_{2D}$ is valid. This approximation is reasonable because one can expect that the zero-point vibrational energy differences between the initial state and transition state are similar for 1° and 2° C-H(D) bond cleavage. The branching ratio for the d_6 isotopologue may thus be written as,

$$f_6 = \frac{k_{1D}}{k_d} + \frac{k_{2H}}{k_d} = p_1 f_{10} + p_2 f_0 \qquad (5)$$

Finally, since $p_1 + p_2 = 1$, the probability for 1° C-H bond cleavage can be expressed in the terms of branching ratios by the following equation,

$$p_1 = \frac{f_0 - f_6}{f_0 - f_{10}} \qquad (6)$$

We emphasize that the approximations that were made to obtain Equation (6) should have only a minimal impact on the accuracy of the analysis. For example, based on characteristic frequencies for molecule-surface vibrations as well as 1° vs. 2° C-H bond stretching, we estimate that our simplifying approximations neglect energy differences of only about 0.2 kJ/mol. This value lies within the uncertainty limits of our data analysis and is more than a factor of ten lower than the difference in activation energies for primary and secondary C-H cleavage that we determined from our data, as discussed in the manuscript.

To estimate p_1 values from the TPRS data, we equate the dissociated fraction obtained during a TPRS experiment with a dissociation probability $\langle S_j \rangle$ that is “averaged” over the range of temperature and coverage that the n-butane precursors react and desorb during TPRS. We then use the $\langle S_j \rangle$ values to calculate average branching ratios and $\langle p_1 \rangle$ values as a function of the initial n-butane coverage. We have recently employed this same approach to estimate apparent probabilities for 1° C-H bond cleavage of propane on PdO(101) based on TPRS data.[2] We set the molecular adsorption probability equal to unity when calculating $\langle f_j \rangle$ values from the dissociated fractions $\langle S_j \rangle$ determined from the TPRS data. This assumption considers that the initial n-butane coverage in the α_1 state is established when the n-butane layer is being prepared at 90 K, rather than by a competitive process wherein weakly-bound species either convert to the α_1 state or desorb as the sample warms during the TPRS measurement.

Computational Details

We used dispersion-corrected density functional theory (DFT-D3) to investigate the activation of n-butane on the PdO(101) surface. The DFT-D3 method is a combination of conventional DFT calculations implemented through the Vienna *ab initio* simulation package[3-5] and the dispersion technique (D3) developed by Grimme *et al*.[6, 7] The DFT-D3 method involves computing dispersion effects separately and adding the dispersion energies and forces (E_{disp}, F_{disp}) to the energies and forces determined through conventional DFT electronic relaxations (E_{dft}, F_{dft}). The total ionic forces $(F_{dft} + F_{disp} = F_{dft-d3})$ are relaxed using a limited memory Broyden-Fletcher-Goldfarb-Shanno optimization method[8] until the forces on all unconstrained atoms are less than 0.01 eV/Å. The parameters used in the DFT calculations are the same as those used in our earlier studies of the PdO(101) surface.[9-12] Projector augmented wave (PAW) pseudo potentials[13] provided in the VASP database are used along with the Perdew-Burke-Ernzerhof (PBE) exchange correlation functional[14] and a plane wave cutoff of 400 eV. Energy calculations to determine E_{dft} are done using the residual minimization method with direct inversion in the iterative subspace for electronic relaxations accelerated using Methfessel-Paxton Fermi-level smearing[15] with a Gaussian width of 0.1 eV. Parameters for calculating the dispersion energy (E_{disp}) have been directly taken from the most recent implementation of dispersion in DFT calculations by Grimme *et al*.[6]

We derive the computational model of the PdO(101) surface by slicing bulk crystalline PdO along the (101) plane, followed by straining the model to match the lattice parameters reported by low energy electron diffraction experiments ($a = 3.057$ Å, $b = 6.352$ Å).[16, 17] The bulk terminated PdO(101) surface is defined by a rectangular unit cell where the $\bar{a}$ and $\bar{b}$ lattice vectors correspond to the $[010]$ and $[\bar{1}01]$ directions of the PdO crystal, respectively (Figure 2). The strained model is relaxed after fixing the bottom layer for stability. The computational model of the PdO(101) surface used in our studies consists of four layers totaling a thickness of ~9 Å and omits the Pd(111) metal substrate. Our earlier studies show that a thickness of 9 Å is sufficient to ignore the metal substrate as increasing the layer thickness does not affect the interaction between the chemisorbing species and the surface. The supercell has a vacuum spacing of ~20 Å normal to the surface in order to eliminate spurious periodic interactions in this direction. A $4 \times 2 \times 1$ Monkhorst-Pack k-point mesh has been used for the 4×1 unit cell sizes which are derived by quadrupling the unit cell size along $\bar{a}$.

The adsorption/binding energies of n-butane are based on a single molecule (kJ/mol C_4H_{10}) chemisorbed on a 4 × 1 PdO(101). The binding energy is defined as

$$E = [E_{bare} + E_{iso}] - E_{chemisorb} \qquad (7)$$

where, E_{bare}, E_{iso} and $E_{chemisorb}$ are the total energies of the bare PdO(101) surface, an isolated n-butane molecule and the chemisorbed molecule/surface system. The periodic images of the n-butane σ-complex in the supercell are separated by more than 6 Å and thus interact only weakly with one another. The n-butane configurations determined on the surface are confirmed to be true minima by performing normal mode analyses, where the frequencies of the vibrational modes are calculated by fixing the surface atoms while leaving the n-butane molecule unconstrained. We use the computed vibrational frequencies to calculate zero-point corrections for the total energies. We computed C-H bond activation pathways for n-butane using the climbing nudged elastic band (NEB) method, and performed normal mode analysis on the transition states to confirm the presence of a single imaginary frequency. In our geometrical optimizations and NEB calculations, we fix the bottom layer of the PdO(101) slab in order to retain the bulk structure but allow all other degrees of freedom of the solid and the n-butane molecule to fully relax. Charge analysis of chemisorbed butane on PdO(101) involves analyzing the net charge on each methyl (CH_n) group. Charges for each CH_n group are obtained by summing atomic charges as determined using the density derived electrostatic and chemical (DDEC) charge analysis reported by Manz and Sholl.[18]

Pathway for 1° vs. 2° C-H bond cleavage of n-butane on PdO(101)

Figure S1 shown below depicts the energy pathways for 1° vs. 2° C-H bond cleavage of the n-butane η^1 complex on PdO(101) as determined by DFT-D3 as well as images of the initial, transition and final state structures. The zero of energy is taken as a gas-phase n-butane molecule plus the bare PdO(101), and the energies are corrected for zero-point vibrational energy. Because the n-butane adsorbate is well-separated from its periodic images, the model is representative of low coverages of n-butane on PdO(101). As discussed in the manuscript, DFT-D3 predicts that the barrier for 1° C-H bond cleavage of the n-butane η^1 complex is 4.0 kJ/mol lower than that for 2° C-H bond cleavage, which agrees well with the experimentally determined value of 3.5 kJ/mol. The apparent energy barriers for C-H bond cleavage lie below the gas-phase energy level, with values of 27.8 and 31.8 kJ/mol for 1° vs. 2° C-H bond cleavage. This prediction is consistent with the experimental observation that n-butane dissociation is facile on PdO(101). However, the apparent energy barriers are lower than our experimental estimate by as much as 28%. Overall, these initial DFT-D3 calculations agree well with our experimental findings which reveal a strong preference for 1° C-H bond cleavage in the initial dissociation of n-butane on PdO(101) in the limit of zero coverage.

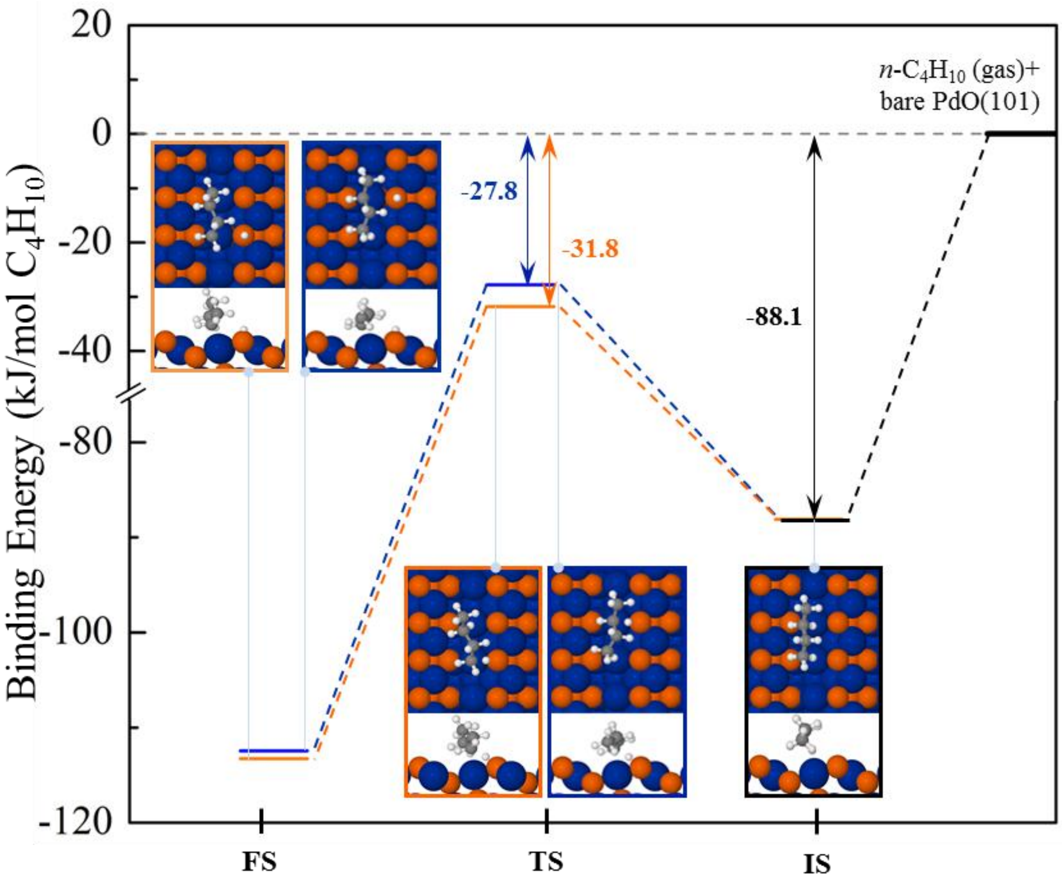

Figure S1. Energy diagram for 1^o and 2^o C-H bond cleavage of the most favored configuration of n-butane on PdO(101). The diagram shows the ZPC energy levels for the IS, TS, and FS for both types of bond cleavage with the isolated n-C_4H_{10} and bare PdO(101) set as zero for reference.

1. W. H. Weinberg and Y. K. Sun, *Science*, 1991, **253**, 542-545.
2. J. F. Weaver, C. Hakanoglu, A. Antony and A. Asthagiri, *J. Am. Chem. Soc.*, 2011, **133**, 16196-16200.
3. G. Kresse and J. Hafner, *Phys. Rev. B*, 1993, **47**, 558-561.
4. G. Kresse and J. Furthmuller, *Comput. Mater. Sci.*, 1996, **6**, 15-50.
5. G. Kresse and J. Furthmuller, *Phys. Rev. B*, 1996, **54**, 11169-11186.
6. S. Grimme, J. Antony, S. Ehrlich and H. Krieg, *J Chem Phys*, 2010, **132**, 154104.
7. S. Grimme, *Wires Comput Mol Sci*, 2011, **1**, 211-228.
8. D. Sheppard, R. Terrell and G. Henkelman, *J. Chem. Phys.*, 2008, **128**, 134106-134110.
9. J. F. Weaver, C. Hakanoglu, J. M. Hawkins and A. Asthagiri, *J Chem Phys*, 2010, **132**, 024709.

10. J. F. Weaver, J. A. Hinojosa, C. Hakanoglu, A. Antony, J. M. Hawkins and A. Asthagiri, *Catal Today*, 2011, **160**, 213-227.
11. A. Antony, C. Hakanoglu, A. Asthagiri and J. F. Weaver, *J Chem Phys*, 2012, **136**, 054702.
12. J. A. Hinojosa, A. Antony, C. Hakanoglu, A. Asthagiri and J. F. Weaver, *J Phys Chem C*, 2012, **116**, 3007-3016.
13. G. Kresse and D. Joubert, *Phys. Rev. B*, 1999, **59**, 1758-1775.
14. J. P. Perdew, K. Burke and M. Ernzerhof, *Phys. Rev. Lett.*, 1996, **77**, 3865-3868.
15. M. Methfessel and A. T. Paxton, *Phys. Rev. B*, 1989, **40**, 3616-3621.
16. H. H. Kan and J. F. Weaver, *Surf Sci*, 2008, **602**, L53-L57.
17. H. H. Kan and J. F. Weaver, *Surf. Sci.*, 2009, **603**, 2671-2682.
18. T. A. Manz and D. S. Sholl, *J Chem Theory Comput*, 2010, **6**, 2455-2468.